associated with successful (but not failed) subgroups of initiators (fig. S4). Thus, failed initiators ultimately move in the direction of the majority (away from their original initiation directions), maintaining cohesion with others.

The failure of high-ranking individuals to dominate movement decisions highlights an important distinction between social status and leadership in wild baboons. Although field-based experiments suggest that dominant individuals, when highly motivated, can shape group movement patterns to their advantage (*1*), our results provide evidence that the decision-making process driving day-to-day movement patterns in baboons is fundamentally shared. Our study emphasizes the power of using high-resolution GPS tracking data to uncover the interdependencies of animal movements. In conjunction with the rich individual-level data that long-term observational studies provide, these methods open up a new window into the social dynamics of wild animal groups.

REFERENCES AND NOTES

1. A. J. King, C. M. S. Douglas, E. Huchard, N. J. B. Isaac, G. Cowlishaw, *Curr. Biol.* **18**, 1833–1838 (2008).
2. M. Nagy, Z. Akos, D. Biro, T. Vicsek, *Nature* **464**, 890–893 (2010).
3. I. D. Couzin *et al*., *Science* **334**, 1578–1580 (2011).
4. L. Conradt, C. List, *Philos. Trans. R. Soc. London Ser. B* **364**, 719–742 (2009).
5. D. J. T. Sumpter, J. Krause, R. James, I. D. Couzin, A. J. W. Ward, *Curr. Biol.* **18**, 1773–1777 (2008).
6. L. Conradt, T. J. Roper, *Trends Ecol. Evol.* **20**, 449–456 (2005).
7. A. J. King, G. Cowlishaw, *Commun. Integr. Biol.* **2**, 147–150 (2009).
8. R. W. Byrne, in *On the Move*, S. Boinski, P. A. Garber, Eds. (Univ. of Chicago Press, Chicago, 2000), p. 501.
9. A. J. King, C. Sueur, *Int. J. Primatol.* **32**, 1245–1267 (2011).
10. A. J. King, D. D. P. Johnson, M. Van Vugt, *Curr. Biol.* **19**, R911–R916 (2009).
11. D. L. Cheney, R. M. Seyfarth, *Baboon Metaphysics* (Univ. of Chicago Press, Chicago, 2008).
12. J. B. Silk, *Science* **317**, 1347–1351 (2007).
13. R. M. Sapolsky, *Science* **308**, 648–652 (2005).
14. S. E. Johnson, J. Bock, *Hum. Nat.* **15**, 45–62 (2004).
15. J. Altmann, *Baboon Mothers and Infants* (Univ. of Chicago Press, Chicago, 1980).
16. A. J. King, G. Cowlishaw, *Anim. Behav.* **78**, 1381–1387 (2009).
17. A. J. King, C. Sueur, E. Huchard, G. Cowlishaw, *Anim. Behav.* **82**, 1337–1345 (2011).
18. S. Stueckle, D. Zinner, *Anim. Behav.* **75**, 1995–2004 (2008).
19. S. A. Altmann, *Foraging for Survival: Yearling Baboons in Africa* (Univ. of Chicago Press, Chicago, 1998).
20. Materials and methods are available as supplementary materials on *Science* Online.
21. O. Petit, J. Gautrais, J.-B. Leca, G. Theraulaz, J.-L. Deneubourg, *Proc. Biol. Sci.* **276**, 3495–3503 (2009).
22. I. D. Couzin, J. Krause, N. R. Franks, S. A. Levin, *Nature* **433**, 513–516 (2005).
23. C. Sueur, J.-L. Deneubourg, O. Petit, *Behav. Ecol. Sociobiol.* **64**, 1875–1885 (2010).

ACKNOWLEDGMENTS

We thank the Kenya National Science and Technology Council, Kenyan Wildlife Service, and Mpala Research Centre for permission to conduct research. All procedures received Institutional Animal Care and Use Committee approval (2012.0601.2015). We thank M. Wikelski, E. Bermingham, D. Rubenstein, and M. Kinnaird for logistical support; R. Kays, S. Murray, M. Mutinda, R. Lessnau, S. Alavi, J. Nairobi, F. Kuemmeth, W. Heidrich, and I. Brugere for assistance; and T. Berger-Wolf, J. Silk, J. Fischer, B. Sheldon, L. Aplin, D. Pappano, M. Grobis, B. Rosenthal, A. Hein, B. Ziebart, L. Polansky, and J. Li for feedback. We acknowledge funding from NSF (grant EAGER-IOS-1250895), the Max Planck Institute for Ornithology, the Smithsonian Tropical Research Institute, and Princeton University. A.S.-P. and D.R.F. received additional support from NIH (grant T32HG003284), NSF (a Graduate Research Fellowship to A.S.-P.), and the Biotechnology and Biological Sciences Research Council (grant BB/L006081/1 to B. C. Sheldon). I.D.C. acknowledges support from NSF (grants PHY-0848755, IOS-1355061, and EAGER-IOS-1251585), the Office of Naval Research (grants N00014-09-1-1074 and N00014-14-1-0635), the Army Research Office (grants W911NG-11-1-0385 and W911NF-14-1-0431), and the Human Frontier Science Program (grant RGP0065/2012). Data are deposited at www.datarepository.movebank.org/ (doi.org/10.5441/001/1.kn0816jn).

SUPPLEMENTARY MATERIALS

www.sciencemag.org/content/348/6241/1358/suppl/DC1
Materials and Methods
Supplementary Text
Figs. S1 to S9
Table S1
References (*24*–*30*)
Movies S1 and S2

16 December 2014; accepted 20 April 2015
10.1126/science.aaa5099

SIGNAL TRANSDUCTION

Structural basis for nucleotide exchange in heterotrimeric G proteins

Ron O. Dror,[1]*†‡ Thomas J. Mildorf,[1]* Daniel Hilger,[2]* Aashish Manglik,[2] David W. Borhani,[1] Daniel H. Arlow,[1]§ Ansgar Philippsen,[1] Nicolas Villanueva,[3] Zhongyu Yang,[4] Michael T. Lerch,[4] Wayne L. Hubbell,[4] Brian K. Kobilka,[2] Roger K. Sunahara,[3]|| David E. Shaw[1,5]†

G protein–coupled receptors (GPCRs) relay diverse extracellular signals into cells by catalyzing nucleotide release from heterotrimeric G proteins, but the mechanism underlying this quintessential molecular signaling event has remained unclear. Here we use atomic-level simulations to elucidate the nucleotide-release mechanism. We find that the G protein α subunit Ras and helical domains—previously observed to separate widely upon receptor binding to expose the nucleotide-binding site—separate spontaneously and frequently even in the absence of a receptor. Domain separation is necessary but not sufficient for rapid nucleotide release. Rather, receptors catalyze nucleotide release by favoring an internal structural rearrangement of the Ras domain that weakens its nucleotide affinity. We use double electron-electron resonance spectroscopy and protein engineering to confirm predictions of our computationally determined mechanism.

G protein–coupled receptors (GPCRs), which represent the largest class of drug targets, trigger cellular responses to external stimuli primarily by activating heterotrimeric G proteins: An activated GPCR, upon binding an inactive, guanosine diphosphate (GDP)–bound G protein, dramatically accelerates GDP release, thus allowing guanosine triphosphate (GTP) to bind spontaneously to the vacated nucleotide-binding site (*1*, *2*). This nucleotide exchange initiates G protein–mediated intracellular signaling. Despite breakthroughs in GPCR structure determination (*3*–*5*), key aspects of the molecular mechanism by which GPCRs accelerate GDP release remain unresolved.

Heterotrimeric G proteins undergo a dramatic conformational change upon binding activated GPCRs (Fig. 1, A and B). Double electron-electron resonance (DEER) spectroscopy has demonstrated that the Ras and helical domains of the G protein α subunit (Gα), which tightly sandwich the nucleotide in all nucleotide-bound G protein crystal structures, separate by tens of angstroms upon GPCR binding and GDP release (*6*). A crystal structure of a GPCR–G protein complex (*4*), and accompanying deuterium-exchange and electron microscopy data (*7*, *8*), confirmed this dramatic domain separation.

These observations have raised several unresolved questions (*4*, *9*). What is the role of domain separation in GDP release? Does a GPCR catalyze GDP release by forcing the domains to separate, or does the GPCR force out GDP, with the absence of GDP leading to subsequent domain separation? More generally, what is the structural mechanism by which a GPCR brings about GDP release?

To address these questions, we performed atomic-level molecular dynamics (MD) simulations of heterotrimeric G proteins with and without bound GPCRs. We initiated simulations from crystal structures of nucleotide-bound G protein heterotrimers [in particular, G_i (*10*) and a

[1]D. E. Shaw Research, New York, NY 10036, USA. [2]Department of Molecular and Cellular Physiology, Stanford University School of Medicine, Stanford, CA 94305, USA. [3]Department of Pharmacology, University of Michigan Medical School, Ann Arbor, MI 48109, USA. [4]Jules Stein Eye Institute and Department of Chemistry and Biochemistry, University of California, Los Angeles, CA 90095, USA. [5]Department of Biochemistry and Molecular Biophysics, Columbia University, New York, NY 10032, USA.
*These authors contributed equally to this work. **†Corresponding author. E-mail: ron.dror@deshawresearch.com (R.O.D.); david.shaw@deshawresearch.com (D.E.S.)** ‡Present address: Department of Computer Science, Department of Molecular and Cellular Physiology, and Institute for Computational and Mathematical Engineering, Stanford University, Stanford, CA 94305, USA. §Present address: Biophysics Graduate Group, University of California, Berkeley, CA 94720, USA. ||Present address: Department of Pharmacology, University of California, San Diego, La Jolla, CA 92903, USA.

chimeric G_t (*11*)], including some in which we omitted the cocrystallized nucleotide, GDP (*12*). We also initiated simulations from the only crystal structure of a GPCR–G protein complex [β_2-adrenergic receptor (β_2AR)–G_s] (*4*), which is also the only structure of a nucleotide-free heterotrimeric G protein. The 66 simulations we performed, of lengths up to 50 μs each, are listed in table S1.

In simulations of GDP-bound G protein heterotrimers, the Gα Ras and helical domains—which are tightly apposed in all nucleotide-bound crystal structures—unexpectedly and dramatically separated from one another (Fig. 1C and figs. S1 and S2). These domain-separated conformations recall the extreme open conformation of the nucleotide-free β_2AR-G_s crystal structure (*4*): In both cases, the helical domain rotated as a rigid body (fig. S3) from its nucleotide-bound crystallographic conformation about a loose hinge located on the distal (away from GDP) side of helix αF (fig. S4). In GDP-bound simulations, the helical domain fluctuated between tightly apposed and separated positions. The maximal rotation observed, ~90°, was less extreme

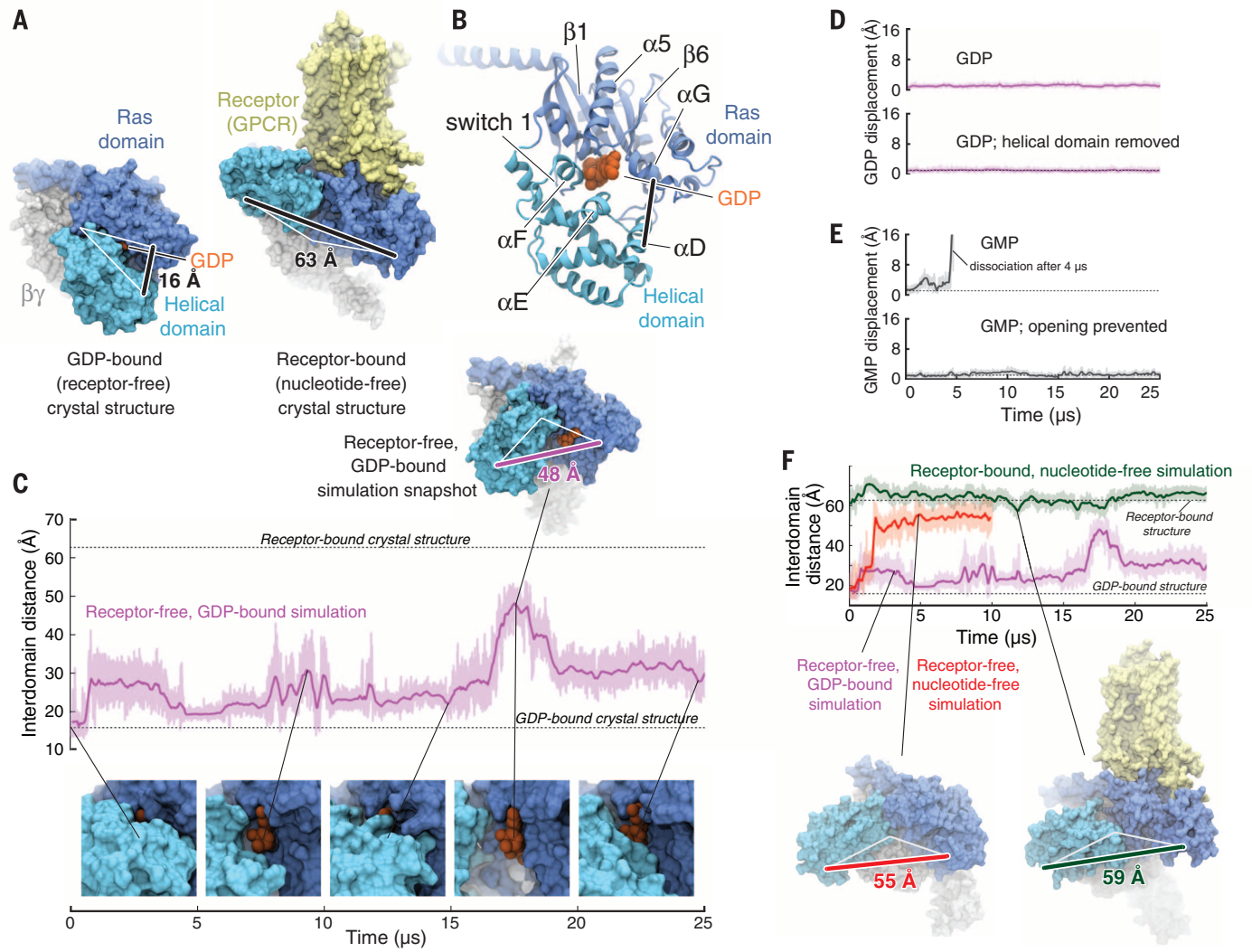

Fig. 1. The Ras and helical domains of the G protein α subunit separate spontaneously and frequently when GDP is bound, even in the absence of a receptor. (**A**) The Ras and helical domains are tightly apposed in all nucleotide-bound G protein crystal structures, enveloping the nucleotide [left: GDP-bound G_t heterotrimer; Protein Data Bank (PDB) entry 1GOT]. Yet they are dramatically separated in the receptor-bound, nucleotide-free structure [right: β_2-adrenergic receptor–G_s heterotrimer (β_2AR-G_s) complex; PDB entry 3SN6]. Orange, GDP; blue, Ras domain; light blue, helical domain; gray, Gβγ; yellow, receptor. The degree of domain separation is represented by a thick black line connecting Ala^{134} and Glu^{272} in $G\alpha_t$ or the corresponding Ala^{161} and Glu^{299} in $G\alpha_s$, with both ends connected by white lines to a pivot point near Thr^{166} ($G\alpha_t$) or Ser^{193} ($G\alpha_s$). (**B**) Key structural motifs of the α subunit, illustrated using the GDP-bound G_t structure. (**C**) Spontaneous domain separation provides an exit pathway for GDP. In simulations of receptor-free, GDP-bound G_t, the Ala^{134}-to-Glu^{272} distance varies substantially as the domains fluctuate between apposed and separated conformations. Raw (light purple) and smoothed (250-ns moving average; dark purple) data are shown. Representative molecular simulation snapshots (top: overview; bottom: nucleotide-binding site) display varying degrees of GDP exposure. Data are from simulation 2 (table S1). (**D**) Domain separation is not sufficient for rapid nucleotide release. GDP remains tightly bound to receptor-free G_t (top), even with the helical domain removed (bottom; traces show displacement of the centroid of the nucleotide nonhydrogen atoms relative to the crystal structure). Data are from simulations 2 and 33. (**E**) Domain separation is necessary for rapid nucleotide release. GMP dissociates spontaneously from receptor-free G_t (top) but remains bound when the interdomain distance is artificially restrained to prevent domain separation (bottom). Data are from simulations 16 and 31. (**F**) Domain separation is greater in the absence of a nucleotide. In simulations initiated from the receptor-free, GDP-bound G_t crystal structure, but with the GDP removed, the Ras and helical domains exhibited extensive and prolonged separation (red trace; left-hand snapshot). In simulations of the β_2AR-G_s complex, also nucleotide-free, the helical domain remained widely separated from the Ras domain, although it typically moved away from the membrane toward the β-propeller of Gβγ (green trace; right-hand snapshot). GDP-bound G_t simulation data from (C) are replicated for reference (purple trace). See the supplementary materials for details on structural renderings. Data are from simulations 2, 14, and 22.

than the nearly 150° rotation of the β_2AR-G_s structure. Nonetheless, the rotation observed in simulation, and the accompanying domain separation of up to ~30 Å (Fig. 1C), dramatically disrupted the interdomain nucleotide-binding site. Such domain separation is particularly notable because it occurred with GDP bound and in the absence of a receptor. Smaller interdomain motions have previously been observed in shorter MD simulations, including some with GDP bound (*13*–*17*).

Despite this substantial domain separation, GDP remained bound throughout our multimicrosecond simulations (Fig. 1D and fig. S5), held in place by persistent, tight contacts with the Ras domain (fig. S4); the few contacts with the helical domain appeared to be weaker, occasionally breaking and reforming. GDP also remained bound to the Ras domain in a simulation with the entire helical domain deleted (Fig. 1D and fig. S5), in accord with the experimental finding that the Ras domain alone is sufficient to bind nucleotides (*18*).

The Gα domain separation observed in simulations cleared an exit pathway for the bound nucleotide, eliminating steric barriers to its escape (fig. S6). Guanosine monophosphate (GMP), which forms fewer contacts with the Ras domain and has a G protein–binding affinity five to six orders of magnitude weaker than that of GDP (*7*), consistently dissociated within microseconds in simulations (Fig. 1E and fig. S5). GMP dissociated only when the domains had separated (fig. S7), however, and when we prevented such separation by restraining the interdomain distance, GMP remained bound (Fig. 1E and fig. S5). Loosening the restraint to permit partial domain separation of ~25 Å was sufficient to allow GMP dissociation (fig. S5).

Lack of a bound nucleotide further promoted domain separation. In nucleotide-free simulations—still initiated from the tightly closed, GDP-bound conformation in the absence of a receptor—domain separation was more dramatic and persistent (Fig. 1F and fig. S1), approaching the level observed in the β_2AR-G_s structure. This increased separation appeared to be due to the loss of nucleotide contacts with residues in and near the helical domain αF helix. αF generally remained in contact with the Ras domain α1 helix when GDP was bound but readily separated from α1 in nucleotide-free simulations, adopting much the same position as in the β_2AR-G_s structure (fig. S8).

In simulations initiated from the β_2AR-G_s structure, which also lacks a bound nucleotide, the domains consistently remained well separated (Fig. 1F and fig. S1). The helical domain adopted conformations similar to those observed in receptor-free, nucleotide-free simulations.

Our nucleotide-bound G protein simulations indicate that a certain degree of Gα domain separation is necessary to clear an exit pathway for nucleotide release. Adequate separation occurs frequently and spontaneously even in the receptor-free, GDP-bound state, but separation alone is not sufficient for rapid GDP release. Rather, a weakening of nucleotide–Ras domain contacts also appears necessary. These observations suggest that an activated receptor could accelerate nucleotide release simply by favoring conformational changes in the Ras domain that weaken its interactions with GDP; the receptor need not promote further domain separation. Prior studies have indicated that binding of an activated receptor promotes Ras domain conformational changes, particularly in the C-terminal α5 helix but possibly also near the Gα N terminus (*4*, *7*, *19*–*22*).

To investigate the nature of such conformational changes and how they might affect nucleotide affinity, we compared our simulations of receptor-free G proteins with and without bound GDP, focusing on those structural elements known to interact with receptors. Our guiding thesis was that a conformation that favors GDP release should itself be favored by the absence of GDP; that is, if affinity for GDP is weaker when the G protein adopts a particular conformation than when it does not, then removal of GDP will increase the equilibrium population of that conformation (fig. S9).

Of the G protein structural elements that contact the receptor in the β_2AR-G_s crystal structure, only the Ras domain α5 helix displayed clear conformational differences between simulations with and without bound GDP (fig. S10). In the absence of GDP, α5 often moved away from the

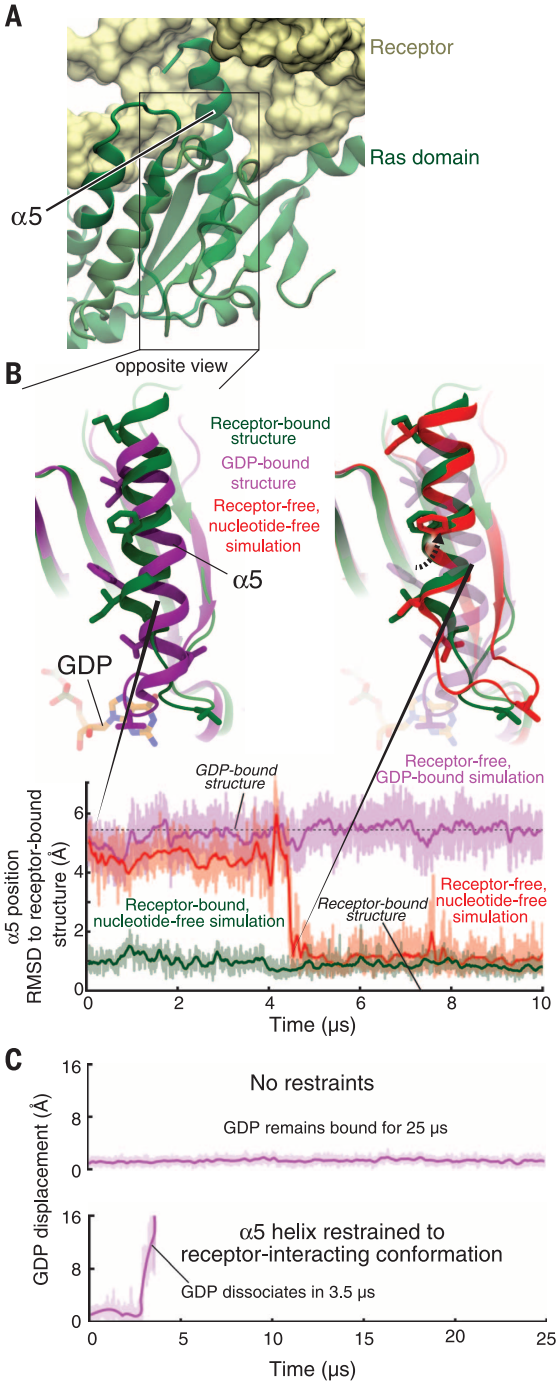

Fig. 2. Receptor-induced displacement of the Gα C-terminal α5 helix disrupts key GDP contacts, thereby promoting nucleotide release. (**A**) In the receptor-bound, nucleotide-free crystal structure (PDB entry 3SN6), α5 docks into the receptor. (**B**) (Top, left) Superimposition of receptor-free, GDP-bound (PDB entry 1GOT; purple) and receptor-bound, nucleotide-free (PDB entry 3SN6; green) crystal structures shows the displacement of α5, relative to the rest of the Ras domain, that occurs when a G protein binds to an activated receptor. (Top, right) In a simulation initialized from a receptor-free, GDP-bound G_t structure but with GDP removed (red), α5 spontaneously rotated 60° and translated 5 Å, adopting a position distal from the nucleotide-binding site that closely matched that of the β_2AR-G_s complex (green). Several side chains in the α5 helix and α5-β6 loop are shown to facilitate comparison between structures. (Bottom) The position of α5 in this simulation (red) changed abruptly at ~4.5 μs to match that of the β_2AR-G_s complex. The α5 position was stable in simulations of receptor-free, GDP-bound G_t (purple) and of the β_2AR-G_s complex (green). Data are from simulations 5, 12, and 22 (table S1). RMSD, root mean square deviation. (**C**) Forcing α5 into the distal conformation accelerates nucleotide release in simulation. TAMD simulations allow observation of GDP release on computationally accessible time scales, but only when α5 is restrained to the distal conformation (i.e., the conformation observed in the β_2AR-G_s complex). Receptor-free, GDP-bound G_t was simulated without (top) or with (bottom) restraints on α5 (see supplementary materials). GDP displacement is measured as in Fig. 1. Data are from simulations 55 and 56.

nucleotide-binding site (~5 Å translation along and ~60° rotation around the helical axis), adopting a conformation closely matching that observed in the β_2AR-G_s structure (*4*), as well as in a rhodopsin-G_i model (*19*) (Fig. 2, A and B, and figs. S10 and S11). The shift to this distal α5 conformation was facilitated by the increased mobility of the adjacent β6-α5 loop in the absence of a nucleotide; this loop directly contacts bound GDP and shifts position in its absence (fig. S12). In receptor-free simulations, the distal α5 conformation was ~1000 times more prevalent in the absence of GDP than in its presence (fig. S10).

Our simulations thus indicate that a repositioning of α5 reduces the affinity of bound GDP. This α5 motion shifts the β6-α5 loop away from the guanine ring of GDP, thereby weakening its contacts with the Ras domain. Previous computational and experimental work has shown that the distal α5 conformation is favored by the activated receptor (*19*); the β_2AR-G_s crystal structure shows that only when α5 is distally positioned can it dock fully into the receptor (*4*) (fig. S13). The distal α5 conformation, adopted only rarely in our simulations of a receptor-free, GDP-bound G protein (fig. S10), apparently becomes the dominant conformation once the G protein binds an activated receptor (*19*), thus facilitating GDP dissociation.

Mimicking the effect of the receptor by restraining the α5 helix to the distal conformation substantially accelerated GDP release in temperature-accelerated MD (TAMD) simulations (Fig. 2C and fig. S14). Release of GDP led to increased domain separation, but the receptor-mimicking restraints were not observed to increase domain separation before GDP release, suggesting that a receptor accelerates nucleotide release primarily by weakening the Ras domain's nucleotide affinity rather than by favoring domain separation.

Our simulations thus suggest the following nucleotide-exchange mechanism. The Ras and helical domains of GDP-bound Gα separate spontaneously, even in the absence of a receptor (Fig. 3). Such separation is necessary but not sufficient for rapid GDP release. Binding of an activated receptor favors conformational changes within the Ras domain (rotation and translation of the α5 helix away from the nucleotide-binding site, leading to rearrangement of the adjacent β6-α5 loop) that weaken its interactions with GDP, thereby enabling GDP to unbind when the helical and Ras domains spontaneously separate. Because GDP helps stabilize closed domain conformations, nucleotide dissociation shifts the equilibrium toward conformations with the two domains widely separated.

Our computationally determined mechanism predicts that the Ras and helical domains separate spontaneously and frequently, even with GDP bound and in the absence of a receptor. Although no crystal structure of a nucleotide-bound G protein has captured a domain-separated conformation—perhaps because such conformations are less populated and less amenable to crystallization than one with the domains in tight contact—the DEER spectroscopy study that originally demonstrated domain separation upon receptor binding also noted a small peak at large distances in GDP-bound G_i interdomain distance distributions [figure 1 of (*6*)].

To better characterize this peak, we performed improved DEER experiments by using a G_i construct with no inserted purification tags (to avoid altering protein dynamics), substantially longer dipolar evolution times (to increase confidence in the measured distance distribution at large distances), and an experimental protocol that delivers an improved signal-to-noise ratio (*12*). We also performed similar experiments on G_s. In both GDP-bound G_i and GDP-bound G_s, we found clear evidence for a minority population exhibiting substantial domain separation (Fig. 4A and fig. S15). The results of a recently

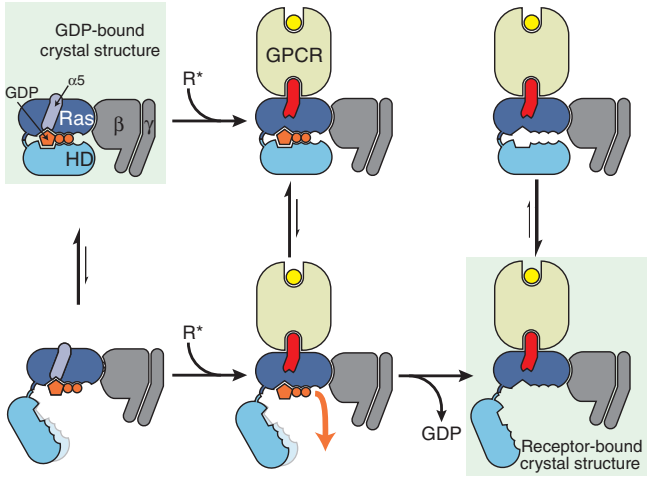

Fig. 3. Proposed mechanism of receptor-catalyzed nucleotide release. (**Left**) The Ras and helical domains (Ras and HD) separate frequently, even in the absence of a receptor, but such separation does not usually lead to GDP release. This rapid (relative to overall GDP release) equilibrium favors the closed conformation (top). (**Middle**) Binding of an activated receptor (R*) favors a Ras domain conformational change—displacement of α5 away from GDP—that weakens interactions between GDP and the Ras domain, allowing GDP to escape when the Gα domains happen to spontaneously separate (bottom). (**Right**) Loss of GDP shifts the equilibrium toward Gα conformations with widely separated domains (bottom).

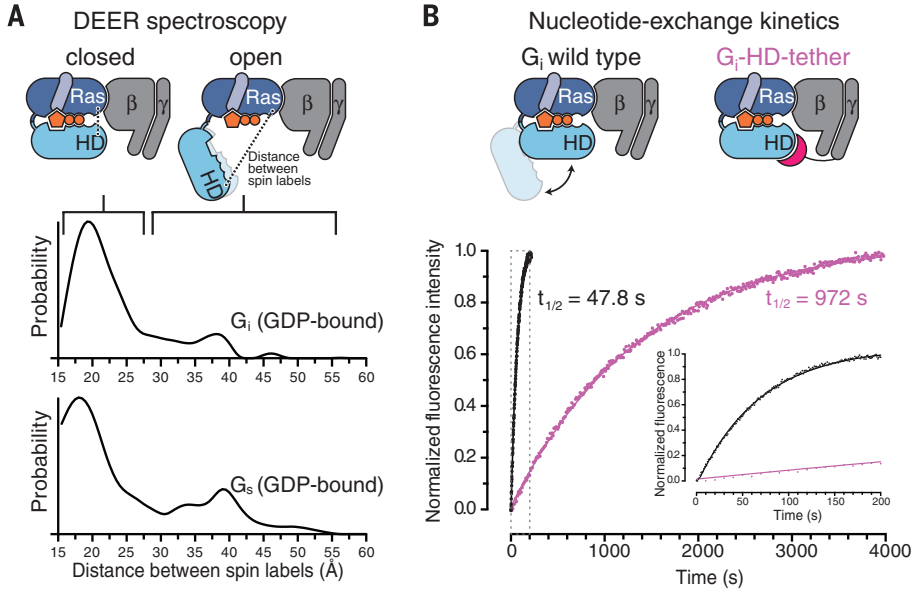

Fig. 4. Experimental validation of spontaneous Gα domain separation in GDP-bound heterotrimeric G proteins and its role in nucleotide exchange. (**A**) DEER distance distributions measured between spin labels attached to the Ras and helical domains of G_i (Glu^{238} and Arg^{90}) and G_s (Asn^{261} and Asn^{112}) show multiple distance peaks, consistent with an equilibrium between closed and open conformations of the α subunit in the presence of GDP, despite the absence of an activated receptor. These distance distributions extend to much larger values than would be expected if the G proteins maintained their crystallographic nucleotide-bound conformations (fig. S15). (**B**) Domain separation affects the basal GDP release rate. The G_i-HD-tether construct (fig. S16), designed to restrict domain separation, exchanges nucleotides 20 times more slowly than the G_i wild type, under conditions where GDP release is rate-limiting. GDP release was monitored by BODIPY-GTPγS binding kinetics, shown for the G_i wild type (black) and G_i-HD-tether (purple). The inset corresponds to the gray dashed box.

published DEER study on GDP-bound $G\alpha_{i1}$ in the absence of the βγ subunit also suggest a minority population with separated domains (*23*).

Our simulations suggest that the minority domain-separated population in GDP-bound G proteins arises due to rapid fluctuations between closed and open conformations and that this spontaneous opening plays an essential role in nucleotide exchange. This implies that constraining domain opening would substantially slow basal nucleotide exchange and, in particular, GDP release. To test this prediction, we engineered a G_i variant to restrict domain opening. In this construct, the N terminus of the γ subunit was fused to a peptide fragment designed to bind the helical domain without impinging on either the nucleotide-binding site or the Ras domain (fig. S16). Binding kinetics measured by fluorescence quenching showed that this helical domain tether slowed basal nucleotide exchange by a factor of 20, under conditions in which GDP release is rate-limiting (Fig. 4B).

Our nucleotide-release mechanism is consistent with earlier mutagenesis studies. Point mutations to the Ras domain β6-α5 loop (*24*) accelerate nucleotide exchange in the absence of a receptor substantially more than mutations that weaken contacts between the Ras and helical domains (*25*), suggesting that weakening interactions between β6-α5 and the GDP guanine ring facilitates nucleotide release to a greater extent than does increasing domain separation. Mutations to α5 that energetically favor the distal conformation increase both receptor-catalyzed and basal nucleotide-exchange rates, whereas those disfavoring that conformation decrease nucleotide-exchange rates (*21*) (fig. S10D).

Several caveats are in order. First, because we did not simulate the complete process of receptor–G protein association, we have not determined the sequence of steps by which a receptor couples to a G protein, nor have we addressed the question of whether a G protein might associate with a receptor before receptor activation (*26*–*28*). Second, although our simulations are orders of magnitude longer than previous atomistic G protein simulations, they still lack sufficient length, and perhaps sufficient accuracy, to reliably determine equilibrium populations of the various conformations. However, our simulations strongly imply the existence of certain conformations and dynamical interchange among them. We cannot rule out the possibility that additional conformational changes to the G protein would manifest themselves on longer time scales. Thus, the GPCR might also induce GDP release, in part through other mechanisms, such as displacement of the β1 strand of Gα (*7*). Third, because crystal structures of nucleotide-bound and receptor-bound heterotrimers are not available for the same G protein, our analysis combines data from different G proteins, under the common assumption that their high level of structural homology implies similar functional mechanisms (*1*, *2*).

Why might heterotrimeric G proteins have evolved to fluctuate spontaneously between open and closed conformations? Tight apposition of the Ras and helical domains appears to be essential for efficient hydrolysis of GTP to GDP (*29*). In the closed conformation, the helical domain plays a role similar to that of the GTPase activating proteins (GAPs) required by small G proteins—which contain only a Ras domain—for efficient catalysis (*18*). Conversely, our results suggest that rapid GDP release requires an open conformation. Spontaneous fluctuation of the helical domain position thus provides an elegant solution to the conflicting needs of catalysis and nucleotide release.

REFERENCES AND NOTES

1. W. M. Oldham, H. E. Hamm, *Nat. Rev. Mol. Cell Biol.* **9**, 60–71 (2008).
2. S. R. Sprang, *Annu. Rev. Biochem.* **66**, 639–678 (1997).
3. D. M. Rosenbaum, S. G. F. Rasmussen, B. K. Kobilka, *Nature* **459**, 356–363 (2009).
4. S. G. F. Rasmussen *et al.*, *Nature* **477**, 549–555 (2011).
5. A. J. Venkatakrishnan *et al.*, *Nature* **494**, 185–194 (2013).
6. N. Van Eps *et al.*, *Proc. Natl. Acad. Sci. U.S.A.* **108**, 9420–9424 (2011).
7. K. Y. Chung *et al.*, *Nature* **477**, 611–615 (2011).
8. G. H. Westfield *et al.*, *Proc. Natl. Acad. Sci. U.S.A.* **108**, 16086–16091 (2011).
9. H. G. Dohlman, J. C. Jones, *Sci. Signal.* **5**, re2 (2012).
10. M. A. Wall *et al.*, *Cell* **83**, 1047–1058 (1995).
11. D. G. Lambright *et al.*, *Nature* **379**, 311–319 (1996).
12. Materials and methods are available as supplementary materials on *Science* Online.
13. L. V. Mello, D. M. van Aalten, J. B. Findlay, *Biochemistry* **37**, 3137–3142 (1998).
14. M. A. Ceruso, X. Periole, H. Weinstein, *J. Mol. Biol.* **338**, 469–481 (2004).
15. K. Khafizov, G. Lattanzi, P. Carloni, *Proteins* **75**, 919–930 (2009).
16. M. Louet, D. Perahia, J. Martinez, N. Floquet, *J. Mol. Biol.* **411**, 298–312 (2011).
17. J. C. Jones, A. M. Jones, B. R. Temple, H. G. Dohlman, *Proc. Natl. Acad. Sci. U.S.A.* **109**, 7275–7279 (2012).
18. D. W. Markby, R. Onrust, H. R. Bourne, *Science* **262**, 1895–1901 (1993).
19. N. S. Alexander *et al.*, *Nat. Struct. Mol. Biol.* **21**, 56–63 (2014).
20. R. Onrust *et al.*, *Science* **275**, 381–384 (1997).
21. E. P. Marin, A. G. Krishna, T. P. Sakmar, *J. Biol. Chem.* **276**, 27400–27405 (2001).
22. W. M. Oldham, N. Van Eps, A. M. Preininger, W. L. Hubbell, H. E. Hamm, *Nat. Struct. Mol. Biol.* **13**, 772–777 (2006).
23. N. Van Eps, C. J. Thomas, W. L. Hubbell, S. R. Sprang, *Proc. Natl. Acad. Sci. U.S.A.* **112**, 1404–1409 (2015).
24. T. Iiri, P. Herzmark, J. M. Nakamoto, C. van Dop, H. R. Bourne, *Nature* **371**, 164–168 (1994).
25. E. P. Marin *et al.*, *J. Biol. Chem.* **276**, 23873–23880 (2001).
26. R. Herrmann, M. Heck, P. Henklein, K. P. Hofmann, O. P. Ernst, *J. Biol. Chem.* **281**, 30234–30241 (2006).
27. P. Scheerer *et al.*, *Proc. Natl. Acad. Sci. U.S.A.* **106**, 10660–10665 (2009).
28. M. Elgeti *et al.*, *J. Am. Chem. Soc.* **135**, 12305–12312 (2013).
29. T. Shnerb, N. Lin, A. Shurki, *Biochemistry* **46**, 10875–10885 (2007).

ACKNOWLEDGMENTS

We thank A. Pan for assistance with TAMD, K. Palmo for help with force field parameterization, J. Valcourt and H. Green for advice on figures, and M. Kirk for editorial assistance. Portions of this work were funded by NIH grants R01GM083118 (B.K.K. and R.K.S.) and R01EY05216 (W.L.H.), the Jules Stein Professor Endowment (W.L.H.), National Eye Institute Core Grant P30EY00331 (W.L.H.), and a Research to Prevent Blindness unrestricted grant (to the Jules Stein Eye Institute). D.H. was supported by the German Academic Exchange Service (DAAD). Author contributions: R.O.D. conceived this study and, with D.E.S., oversaw MD simulations and analysis. R.O.D., T.J.M., and D.H.A. designed MD simulations. T.J.M. performed MD simulations and, with D.W.B., modeled proteins based on crystal structures. T.J.M. analyzed MD simulations, with guidance from R.O.D. T.J.M. and A.P. performed molecular visualization. D.H. developed a minimal cysteine construct for G_s, prepared spin-labeled protein, and assisted Z.Y. and M.T.L. in obtaining and analyzing DEER data. A.M. and D.H. designed the HD-tether construct, and A.M. performed the kinetics experiments. W.L.H. and B.K.K. supervised experimental work. R.O.D., T.J.M., N.V., and R.K.S. interpreted and synthesized data. R.O.D., T.J.M., D.W.B., and D.E.S. wrote the manuscript, with input from D.H., A.M., B.K.K., and R.K.S. R.O.D. and D.E.S. supervised the overall research.

SUPPLEMENTARY MATERIALS

www.sciencemag.org/content/348/6241/1361/suppl/DC1
Materials and Methods
Figs. S1 to S17
Table S1
References (*30*–*58*)

18 December 2014; accepted 15 May 2015
10.1126/science.aaa5264

PROTEIN DESIGN

Design of ordered two-dimensional arrays mediated by noncovalent protein-protein interfaces

Shane Gonen,[1,2,3,4] Frank DiMaio,[2,3] Tamir Gonen,[1]* David Baker[2,3,4]*

We describe a general approach to designing two-dimensional (2D) protein arrays mediated by noncovalent protein-protein interfaces. Protein homo-oligomers are placed into one of the seventeen 2D layer groups, the degrees of freedom of the lattice are sampled to identify configurations with shape-complementary interacting surfaces, and the interaction energy is minimized using sequence design calculations. We used the method to design proteins that self-assemble into layer groups P 3 2 1, P 4 2_1 2, and P 6. Projection maps of micrometer-scale arrays, assembled both in vitro and in vivo, are consistent with the design models and display the target layer group symmetry. Such programmable 2D protein lattices should enable new approaches to structure determination, sensing, and nanomaterial engineering.

Programmed self-assembly provides a route to patterning matter at the atomic scale. DNA origami methods (*1*, *2*) have been used to generate a wide variety of ordered structures, but progress in designing protein assemblies has been slower owing to the greater complexity of protein-protein interactions. Biology provides a number of examples of ordered two-dimensional (2D) protein arrays: Bacterial S-layer proteins assemble into